**Proceedings of the 7th GACM Colloquium on Computational Mechanics
for Young Scientists from Academia and Industry
October 11-13, 2017 in Stuttgart, Germany**

Preliminary calibration of a phase-field model for cracks due to shrinkage in cement-based materials

Tuanny Cajuhi[1]*, Pietro Lura[2] and Laura De Lorenzis[1]

Micro Abstract
Shrinkage in cement-based materials can lead to early microcracking. The phenomenon is related to the change of volume at early states, which can lead to cracking if the medium is either internally or externally restrained. Objective of this work is to describe drying shrinkage and autogenous shrinkage in cementitious materials within the framework of poromechanics and phase-field modeling with special focus on crack initiation and evolution. A preliminary calibration of the material parameters is performed in this paper.

[1]Institute of Applied Mechanics, Technical University of Braunschweig, Braunschweig, Germany

[2]Swiss Federal Laboratories for Materials Science and Technology, EMPA, Dübendorf, Switzerland

***Corresponding author**: t.cajuhi@tu-braunschweig.de

Introduction

The material properties of cement-based materials such as Young's modulus, tensile strength and fracture energy vary with age (i.e. mainly with the degree of hydration) and moisture content. The numerical modeling of drying phenomena in such materials should take into account the evolution of the properties such that predictions can become more accurate. A framework for numerical modeling of coupled deformation, drying and cracking with the phase-field approach of brittle fracture was presented in [3]. This framework accounts for the evolution of the elastic modulus and the fracture energy, both as functions of the moisture content.

This paper presents a study on the properties of a cementitious material based on previous experimental work [5]. The parameters are used as basis for the calculation of the length scale needed for the phase-field modeling approach and for a prelimininary calibration of the phase-field framework.

1 Material properties

The experimental results shown in this paper are based on the experiments of Di Bella et al. [5]. The properties of a cementitious mortar at $1, 7$ and 91 days are measured with compact tension tests (CTT). The dimensions of the specimen are shown in Fig. 1. Pins with 20 millimeter diameter were inserted in the holes to load the specimen. The mixture proportions are 599kg/m^3 of ordinary, rapid hardening portland cement CEM I 52.5 N, 1331kg/m^3 of sand and 306kg/m^3 of water. The average sand grain size is 312μm and the maximum grain size is 650μm.

Inverse analysis of the force-displacement curves from the CTT is conducted to obtain the elastic modulus, tensile strength and fracture energy. The inverse analysis is based on the hinge model with multi-linear softening curve [8]. The obtained material properties can be found in Table 1.

Age (days)	1	7	91
E (GPa)	18	32	28
σ_t (MPa)	1	1.7	2.2
$\mathcal{G}_c$ (N/m)	16	16	34

Table 1. Elastic and fracture properties of a cementitious material at different ages

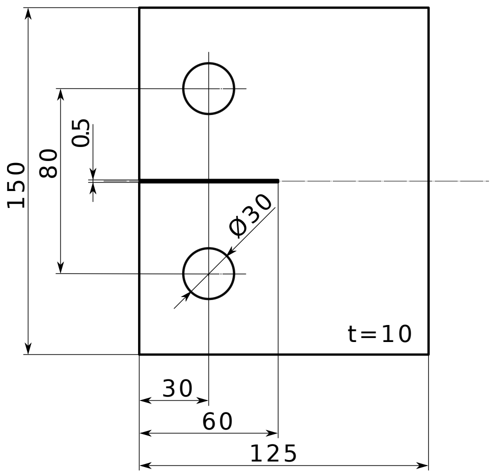

Figure 1. Dimensions of CT specimen expressed in millimeters. The thickness of the specimen is 10 millimeters and the opening is 0.5 millimeter.

2 Computational framework

In order to perform a numerical analysis with the phase-field formulation for brittle fracture, the elastic and fracture properties of the material are needed. The computational framework which serves as basis for this work is presented in detail in Cajuhi et al. [3]. Due to the purely mechanical nature of the current test, only the equilibrium and phase-field equations are considered and the coupling between the mechanical and pore pressure fields is neglected. The equilibrium equation is given as

$$\nabla \cdot ((1-d^2) \cdot \boldsymbol{\sigma}^+ + \boldsymbol{\sigma}^-) = \mathbf{0} \tag{1}$$

where the total Cauchy stress is split into positve $\boldsymbol{\sigma}^+$ and negative $\boldsymbol{\sigma}^-$ contributions, which are due to tensile and compressive loads, respectively. They can be computed by the split of [1]. The variable d represents the crack phase-field that varies from 0 to 1. The limits represent intact and fully broken material, respectively. The crack phase-field is computed by the following phase-field evolution equation

$$\mathcal{G}_c[d - \ell^2 \nabla d] - 2(1-d)\mathcal{H} = 0. \tag{2}$$

The parameters in Eq. (2) are the fracture energy $\mathcal{G}_c$ and the length scale ℓ, which denotes the width of the transition zone of the smeared crack. The maximum energy within the load history is expressed by $\mathcal{H}$ [7]. The energy couples the phase-field evolution equation and the equilibrium equation.

The length scale parameter is computed through $\ell = \left(\dfrac{9}{16}\right)^2 \dfrac{\mathcal{G}_c E}{6\sigma_t^2}$, proposed by Borden et al. [2]. The values from Table 1 are used. The obtained length scales are shown in Table 2.

Age (days)	1	7	91
ℓ (m)	0.012	0.009	0.010

Table 2. Length scale parameter computed at different ages.

3 Analysis results

The Young's modulus, fracture energy and length scale ($\ell = 0.01$m) are used as input in the displacement driven simulations of the CTT. The Poisson's ratio is assigned the value 0.2. In the model, the lowest part of the lower hole is fixed in the horizontal and vertical directions. The displacement increment applied at the highest part of the upper hole is 2×10^{-7}m with fixed horizontal displacement. The numerical scheme is computed using 10 staggered iterations [6]. Figure 2 shows the results of the numerical test with locally refined mesh near the cracking zone.

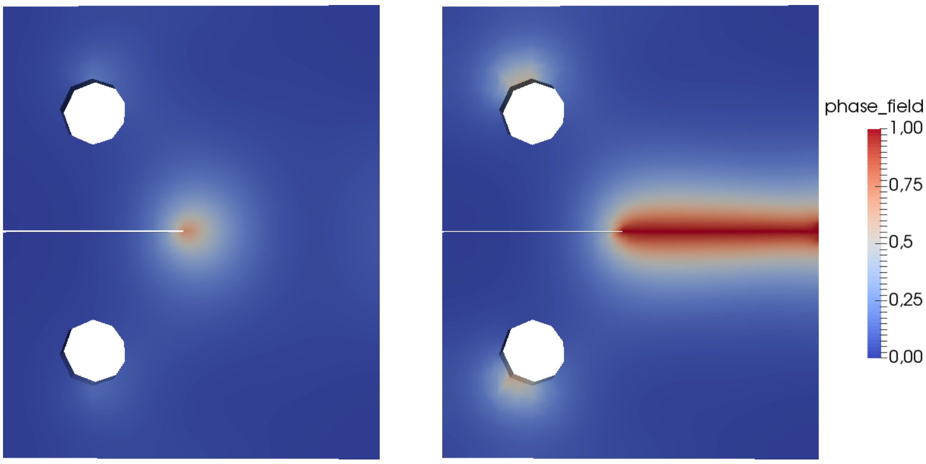

Figure 2. Phase-field results of specimen with 91 days at peak load after 245 load increments and fully propagated crack after 1250 load increments. The mesh size h should satisfy $h \leq \ell/2$ [7]. The mesh is refined with element size 0.25 millimeter near the initial opening and 2 millimeters near the cracking zone.

The maximum splitting forces from the force-displacement curves obtained experimentally $F_{\max}^{\text{exp}}$ and numerically $F_{\max}^{\text{num}}$ for each age are shown in Table 3. The splitting force is computed at the left edge of the specimen. It can be noticed that the maximum splitting forces obtained in the simulations are higher than the experimental values.

Age (days)	1	7	91
$F_{\max}^{\text{exp}}$ (N)	145	232	343
$F_{\max}^{\text{num}}$ (N)	220	299	406
relative error (%)	34	22	15

Table 3. Mixtures and material properties

The differences in the peak load should be investigated further. A reason for discrepancy could be related to the approach used to calibrate the tensile strength and fracture energy in [5, 8] and the approach used in the numerical simulation. The differences could be also related to the strategy used to compute the length scale parameter, which affects the peak load as shown in the study of [4]. From the computational point of view, the number of iterations in the staggered scheme can also affect the peak load. The computational model does not take into account the contact between the pin and the hole and this can affect the obtained splitting load and contribute to the stiffer response. Furthermore, it can be noticed that the error decreases with the age of the specimen, which could be related to the difficulty in measuring the material properties at early ages when the degree of hydration of the cement is low. Further investigations are ongoing.

Conclusions

This work has presented a preliminary investigation on the calibration of the material properties of a cementitious material. The investigation focused on the elastic modulus, fracture energy and tensile strength. The material properties were obtained through inverse analysis based on the hinge-model. The obtained values were used to determine the length scale parameter and as input in the phase-field model of brittle fracture. The CTT specimen was simulated and the maximum splitting force of each age was compared with the experimental results from [5]. The obtained forces in the simulations were 15-34% higher than the experimental ones. The differences could be related to the different approaches used to calibrate the tensile strength and fracture energy in [5, 8] and in the numerical model, the value of the length scale parameter and the oversimplification of the current numerical model which does not account for contact. Further investigations are currently ongoing and experiments are being conducted at the Swiss Federal Laboratories for Materials Science and Technology (Empa) to determine the mechanical and hygral properties of cement-based materials. Once the mechanical properties are calibrated in the model, they will be expressed in terms of age and moisture content and inserted in the poromechanical phase-field framework of [3] to simulate drying and autogenous shrinkage.

Acknowledgements

We would like to acknowledge the funding provided by the German Research Foundation DFG GRK-2075.

References

[1] H. Amor, J.-J. Marigo, and C. Maurini. Regularized formulation of the variational brittle fracture with unilateral contact: Numerical experiments. *J. Mech. Phys. Solids*, 2009.

[2] M. J. Borden, C. V. Verhoosel, M. A. Scott, T. J. Hughes, and C. M. Landis. A phase-field description of dynamic brittle fracture. *Computer Methods in Applied Mechanics and Engineering*, pages 77–95, 2012.

[3] T. Cajuhi, L. Sanavia, and L. De Lorenzis. Phase-field modeling of fracture in variably saturated porous media. *Computational Mechanics*, in print, 2017.

[4] R. de Borst and C. Verhoosel. Gradient damage vs phase-field approaches for fracture: Similarities and differences. *Computer Methods in Applied Mechanics and Engineering*, 312:78 – 94, 2016. Phase Field Approaches to Fracture.

[5] C. Di Bella, A. Michel, H. Stang, and P. Lura. Early age fracture properties of microstructurally-designed mortars. *Cement and Concrete Composites*, 75:62 – 73, 2017.

[6] T. Gerasimov and L. D. Lorenzis. A line search assisted monolithic approach for phase-field computing of brittle fracture. *Computer Methods in Applied Mechanics and Engineering*, 312:276 – 303, 2016. Phase Field Approaches to Fracture.

[7] C. Miehe, F. Welschinger, and M. Hofacker. Thermodynamically consistent phase-field models of fracture: variational principles and multi-field fe implementations. *International Journal for Numerical Methods in Engineering*, 83:1273–1311, 2010.

[8] J. Skoček and H. Stang. Inverse analysis of the wedge-splitting test. *Engineering Fracture Mechanics*, 75(10):3173 – 3188, 2008.